Plasma-Assisted Interface Engineering of Boron Nitride Nanostructure Films

Amir Pakdel,* Yoshio Bando, and Dmitri Golberg*

World Premier International Center for Materials Nanoarchitectonics (WPI-MANA), National Institute for Materials Science (NIMS), 1-1 Namiki, Tsukuba 305-0044, Japan

ABSTRACT Today many aspects of science and technology are progressing into the nanoscale realm where surfaces and interfaces are intrinsically important in determining properties and performances of materials and devices. One familiar phenomenon in which interfacial interactions play a major role is the wetting of solids. In this work we use a facile one-step plasma method to control the wettability of boron nitride (BN) nanostructure films *via* covalent chemical functionalization, while their surface morphology remains intact. By tailoring the concentration of grafted hydroxyl groups, superhydrophilic, hydrophilic, and hydrophobic patterns are created on the initially superhydrophobic BN nanosheet and nanotube films. Moreover, by introducing a gradient of the functional groups, directional liquid spreading toward increasing [OH] content is achieved on the films. The resulting insights are meant to illustrate great potentials of this method to tailor wettability of ceramic films, control liquid flow patterns for engineering applications such as microfluidics and biosensing, and improve the interfacial contact and adhesion in nanocomposite materials.

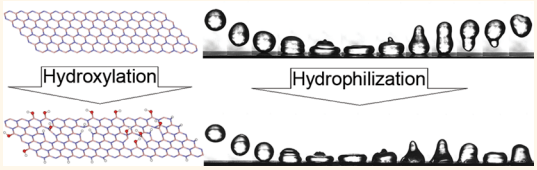

KEYWORDS: boron nitride nanotubes · boron nitride nanosheets · interface engineering · plasma treatment · superhydrophobicity · superhydrophilicity · directional wetting

Surfaces and interfaces occur everywhere in nature, from minute sand grains to the vast expanse of oceans. Surfaces and interfaces play a key role in nanoscience since they often serve as platforms for the growth of low-dimensional materials. Besides, the physical and chemical processes taking place at these regions can be different from the ones in bulk phases, and decisive in controlling the materials performances in diverse areas of applications, such as green energy (fuel cells, solar cells, and hydrogen storage), medicine (biomaterials, biosensors, and gene chips), catalysis, electronics, composites, *etc*. Continuous progress in nanomaterial syntheses and extensive research on interfacial phenomena of low-dimensional materials have brought the advent of a new area of nanoscale interface engineering which aims at employing nanoscale interfacial features to obtain materials with modified or totally new properties. A classical example of interface-related properties is the wettability of materials, where the interfacial interactions between the solid surface and liquid determine the wetting degree. Surface wetting is prevalent in nature featuring various biological surfaces which benefit from specialized structural and chemical modifications to manage the wetting behavior.[1] For example, the superhydrophobic surface of a lotus leave contains nano/micro-roughness that enables self-cleaning, whereas the microscopically smooth superhydrophilic surface of a water plant allows water absorption and water spreading to achieve a sustained state of wetness.[2]

Inspired by nature, topographical surface structuring has been employed to create a multitude of new engineered surfaces with diverse wetting properties. Certain types of such surface structures can even induce directional wetting which allows a great degree of control over liquid spreading.[3−6] In this regard, arrays of symmetric or asymmetric surface features, such as arrays of nanotubes, nanowires, grooves, inclined pillars, and helical protrusions, have shown unique anisotropic wetting properties.[7] Besides morphological changes at the interface, chemical functionalization can also affect the wettability of a surface. Depending on the material properties, a wide range of methods can be used to achieve surface functionalization, such as chemical, electrochemical, and mechanochemical treatments, vapor deposition, and exposure to plasma of

* Address correspondence to PAKDEL.Amir@nims.go.jp, GOLBERG.Dmitri@nims.go.jp.

Received for review July 28, 2014 and accepted October 7, 2014.

Published online October 07, 2014
10.1021/nn5041729

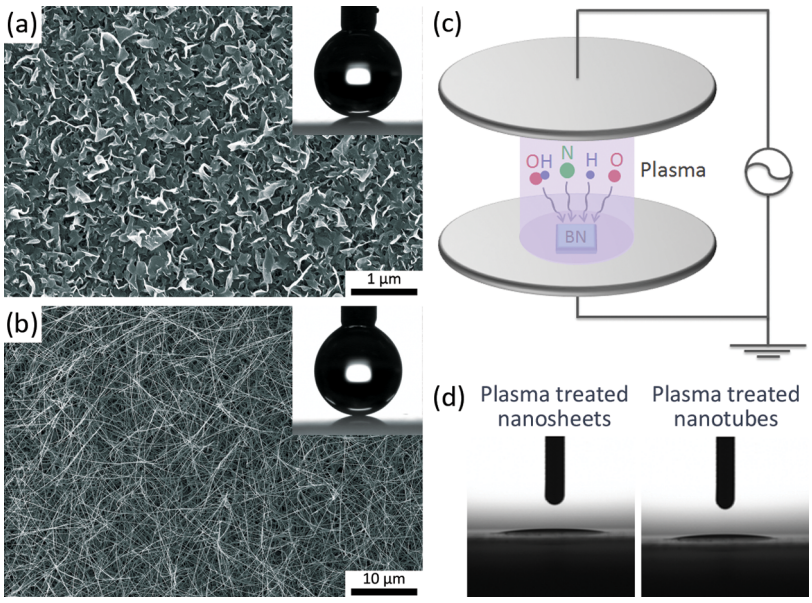

Figure 1. (a,b) SEM images of BN nanosheets and nanotubes grown as uniform films over Si/SiO_2 substrates by a thermal CVD method. The insets show 10 μL water droplets residing on the superhydrophobic BN nanostructure films. (c) Schematics of the air-plasma device in which the samples were subject to direct bombardment of the plasma species. (d) CA measurements after air-plasma treatment indicate that both the BN nanosheet and nanotube films have become superhydrophilic.

accelerated ions and particles.[8−11] Among these techniques, plasma treatment is technologically very important due to its possibility of scaling up to produce large quantities of material necessary for commercial use, its much lower reaction time compared to other functionalization techniques, and the variety of functional groups that can be achieved depending on the plasma parameters.[12]

Low-dimensional boron nitride (BN) materials are among the most promising inorganic nanosystems explored so far because of their unique properties, such as excellent stiffness, high thermal conductivity, outstanding chemical and thermal stability, corrosion resistance, electrical insulation, wide optical bandgap, and deep UV emission.[13,14] Recent studies on hierarchical BN nanostructure surfaces in our group as well as Yap's group of Michigan Technological University and Chen's group of Deakin University showed that nanoscale topography can give an unusual rise to water repelling properties of BN surfaces.[15−19] We synthesized various BN films composed of vertically aligned or randomly oriented 1D and 2D nanostructures by a chemical vapor deposition (CVD) method and investigated the influence of surface morphology on their wetting properties.[17−20] We observed that a smooth BN film is relatively hydrophilic with a water contact angle (CA) of ~50°, whereas nanostructured BN surfaces can be hydrophobic or even superhydrophobic with water CAs larger than 150° (Figure S1, Supporting Information). This CA variation was attributed to the combined effects of surface roughness and partial liquid−solid contact at the interface.

In the present work, chemical functionalization of BN nanostructure films, as another aspect of nanoscale interface engineering to control the wetting properties, is achieved by air-plasma treatment. The resulting hydroxyl-functionalized BN nanosheets and nanotube films show a drastic change in their water-repellency from superhydrophobicity to superhydrophilicity. The mechanisms involved in this one-step functionalization process and their influence on wetting properties are discussed in detail. Moreover, by controlling the interfacial interactions during the plasma treatment, a chemical gradient of hydroxyl groups on the BN nanostructure films is achieved which is then utilized to demonstrate directional-water-spreading functionality of the films. Such a controllable surface chemistry route provides further possibilities in device design for a wide application range from microfluidics and water treatment to nanocomposites and chemical sensing.

RESULTS AND DISCUSSION

Figure 1a,b shows scanning electron micrographs (SEM) of BN nanosheet and nanotube films prepared by the CVD method. Detailed transmission electron microscopy (TEM) studies revealed purity and good crystallinity of the synthesized nanosheets and nanotubes (Figure S2, Supporting Information). The average diameter of the nanotubes was ~60 nm and the nanosheets were mostly 2−5 nm in thickness. Both nanostructured films demonstrated superhydrophobicity with average water CA values of ~153° and ~157° for BN nanosheets and nanotubes, respectively. The films were then subject to direct ion/electron bombardment in an air-plasma device for 10 min, as schematically illustrated in Figure 1c. As a result, their water CA dropped to almost zero (water completely

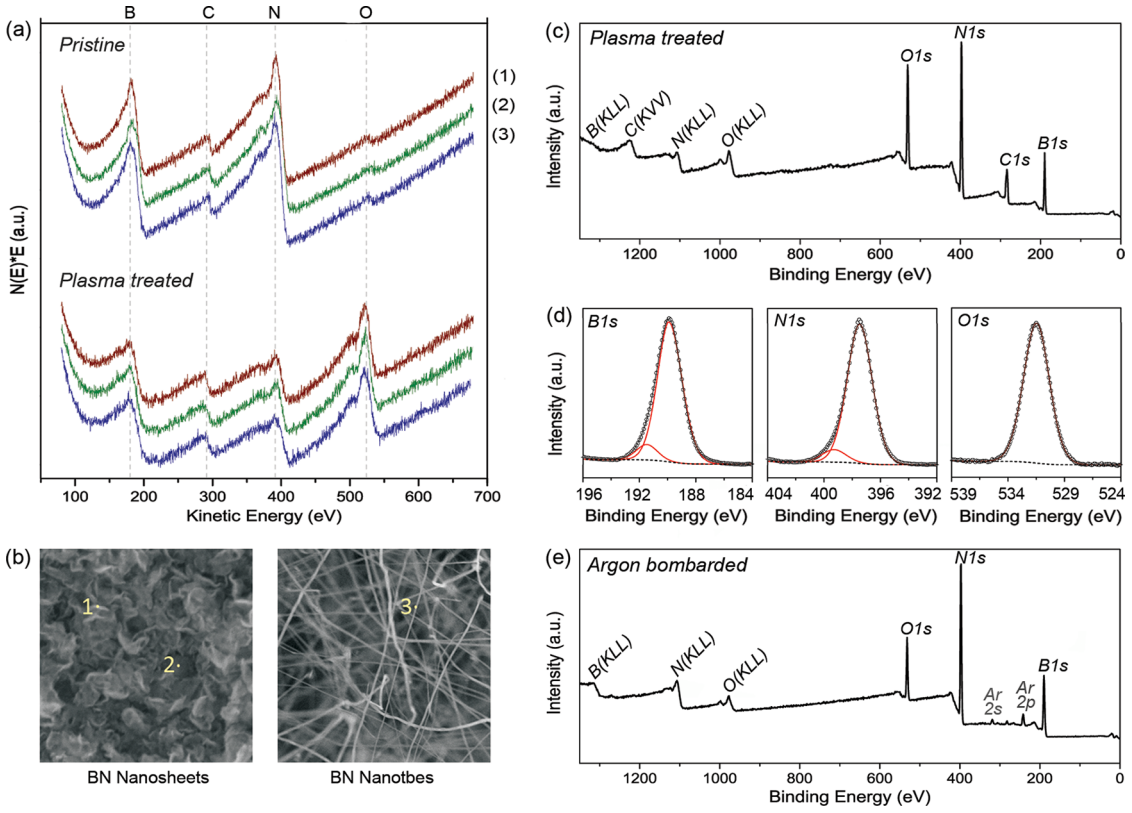

Figure 2. (a) AES spectra taken from the edges (1) and planes (2) of a BN nanosheet and walls of a BN nanotube (3) before and after air-plasma treatment; (b) SEM images of the BN nanostructures indicating the points from which the AES spectra were collected; (c) XPS survey spectrum of BN nanosheets after air-plasma treatment; (d) high-resolution core-level photoemission spectra of boron, nitrogen and oxygen; (e) XPS survey spectrum of BN nanosheets after air-plasma treatment and argon ion sputtering.

spread over the film surfaces) indicating a drastic change in their wetting behavior from superhydrophobicity to superhydrophilicity (Figure 1d). The air-plasma treated BN nanostructure films kept their extreme wettability for several days, and their water CA raised only ~10° after 3 days in ambient conditions, possibly due to the surface adsorption of airborne molecules.[21]

To identify the origins of stable superwettability of plasma-treated hierarchical BN films, several surface characterization techniques were utilized. A comparison between scanning electron micrographs (SEM) before and after the treatment confirmed that the overall morphology of the BN films remained intact during the process (Figure S3, Supporting Information). Figure 2a displays local chemical composition analysis of the BN nanostructures performed by an Auger electron spectrometer (AES) equipped with a secondary electron imaging system (SEM), before and immediately after the air-plasma treatment (time of exposure to the environment was less than 1 min). The red, green, and blue curves are typical spectra gathered from the edge of a nanosheet, the planes of a nanosheet, and the walls of a nanotube, respectively, as indicated in the SEM images of Figure 2b. The untreated nanosheet and nanotube films show two main peaks related to boron and nitrogen and small peaks related to oxygen and carbon, which could be attributed to minuscule levels of impurity and/or airborne molecules on the surface. However, after the plasma treatment, the oxygen level immensely rises in all spectra indicating the possible oxidation/hydroxidation of the BN nanostructures.

To further characterize the chemical state of the surface, X-ray photoelectron spectroscopy (XPS) was carried out on BN nanostructure films. Compared to the localized chemical analysis performed by AES, a large area analysis (~400 μm in diameter) by XPS conveys complementary information about surface bonds. XPS survey spectrum of plasma-treated BN nanosheets (Figure 2c) identifies B 1s, N 1s, O 1s, and C 1s peaks at ~190.1, ~397.6, ~531.6, and ~284.3 eV, respectively. Higher resolution core-level photoemission spectra of the elements (Figure 2d) display some levels of asymmetry and broadening which suggest the existence of more than one type of bonding scheme for the atoms (larger sized spectra available at Figure S4, Supporting Information). The B 1s spectrum in Figure 2d can be fitted by two curves using a Gaussian profile; the main one with a binding energy peak at ~190.0 eV is attributed to B−N bonds and the other one at ~191.8 eV is assigned to B−OH bonds that originate from the hydroxidation of some boron atoms

at the surface of the sample. The B−OH signal is observed at a higher binding energy than the B−N signal owing to higher electronegativity of the hydroxide anion compared to that of nitrogen, and yet in a lower bonding energy than B═O in B_2O_3 (∼193 eV) due to the lower oxidation state in B−OH.[22−24] The N 1s spectrum in Figure 2d can be fitted by two curves; the main one with the binding energy peak centered at ∼397.5 eV is attributed to N−B bonds and the other one centered at ∼399.8 eV refers to N−H bonds.[22−24] The O 1s spectrum in Figure 2d is centered at ∼531.6 eV and indicates the formation of HO−B bonds (hydroxidation of boron). It has a lower value than those of O−Si bonds (532.5 eV) in SiO_2 and O═B bonds (533 eV) in B_2O_3; therefore, it may be interpreted to have originated neither from the substrate nor from higher-state oxidation of boron.[22−25]

To investigate the stability of the hydroxyl functional groups on the BN nanostructure surfaces, argon ion sputtering was performed inside the XPS chamber. Figure 2e shows the XPS survey spectrum of the air-plasma treated BN nanosheet film after argon ion sputtering. It is seen that even after the ion bombardment of the surface, a strong O 1s peak in the spectrum appears which demonstrates the high stability of functional hydroxyl groups on the surface. On the contrary, the intensity of the carbon peak drastically drops implying the removal of loosely bound superficial carbon atoms from the surface. The disappearance of the Auger line at ∼1223 eV also confirms the elimination of carbon atoms after argon bombardment, suggesting that unlike the covalently bound −OH functional groups, carbonaceous species were mainly trapped or physisorbed contaminants on the surface. The new two peaks appearing at ∼321.2 and ∼243.9 eV are attributed to Ar 2s and Ar 2p photoelectrons, respectively, which have resulted from argon ion implantation during the surface bombardment. XPS experiments on BN nanotube films also yielded similar results (Figure S5, Supporting Information).

The detailed AES and XPS analyses of the plasma-treated BN nanostructure films suggest that hydroxyl and hydrogen ions were grafted on the edges and planes of the BN nanosheets and nanotubes, whose functionalization mechanism can be explained as follows. In air-plasma treatment, air molecules (primarily nitrogen, oxygen, and water vapor) become excited and react with other molecules, knock off electrons, and emit photons. The excited nitrogen molecules mainly relax by emission of photons which produce the observable purple light in the plasma region. The excited oxygen molecules on the other hand, are more stable and capable of reacting with other oxygen molecules to form ozone or breaking chemical bonds in water vapor molecules to form reactive [OH], [O], and [H] species. Such reactive ions and radicals can readily react with other chemicals present in air and the nearby BN surface, causing the breakage of existing chemical bonds and formation of new ones. Thus, the functionalization process can include several mechanisms as schematically illustrated in Figure 3a. The covalent bonds can primarily form at the chemically active edges of BN nanosheets and nanotubes as preferred sites to saturate their dangling bonds. In addition, the nanosheet planes and nanotube walls normally contain certain amount of point defects (such as vacancies) serving as active sites for chemical interactions. Moreover, the attack of reactive species on electron-deficient boron and electron-rich nitrogen atoms can result in covalent-bond formation *via* Lewis acid−base interactions, for instance between the hydroxyl groups (as the electron pair donors) and the boron atoms (as the electron pair acceptors with vacant p orbitals). The plasma components (i.e., chemical species and energetic particles) may also attack the B−N bonds, break them, and create new bonds. In this case, the covalent bond formation between a boron atom and a hydroxyl ion or a nitrogen atom and a proton (H^+) occurs with concomitant cleavage of the in-plane B−N bond to satisfy the valence conditions. Consequently, the boron and nitrogen atoms can be expected to become dislocated out of the planar sp^2 lattice as their hybridization is modified to the tetrahedral sp^3 configuration by the functionalization.[25] Then, when the functionalized surface was in contact with water, the polarity of the grafted hydroxyl groups could create a strong attraction to the extremely polar water molecules, resulting in hydrogen bonding, as schematically shown in Figure 3b. Such strong intermolecular forces and dipole moment interactions led to the observed hydrophilic effect, as predicted by theoretical calculations.[26,27] Therefore, the extreme change of wettability from superhydrophobicity to superhydrophilicity in both BN nanosheet and nanotube films after the air-plasma treatment is attributed to the chemical engineering of the interface between the BN nanostructures and water molecules. The obtained results are in agreement with the previous reports on strong hydrophilic behavior of boron hydroxide,[28] compared to the hydrophobic nature of boron oxide[28] and boron nitride.[15−19]

The present one-step plasma-assisted covalent addition of hydroxide and hydrogen ions to boron and nitrogen atoms in BN nanostructures is complementary to the recent multistep methods for hydroxyl group grafting of BN nanosheets and nanotubes *via* ultrasonication assisted hydrolysis, solution-phase radical functionalization, and autoclaved high-temperature high-pressure chemical reactions.[25,29−31] Moreover, the present plasma method enabled us to control the wetting degree of the films by grading the density of the chemical functional groups. This was achieved by using a canopy-shaped physical mask with a small gap, as illustrated in Figure 4a. Such type of

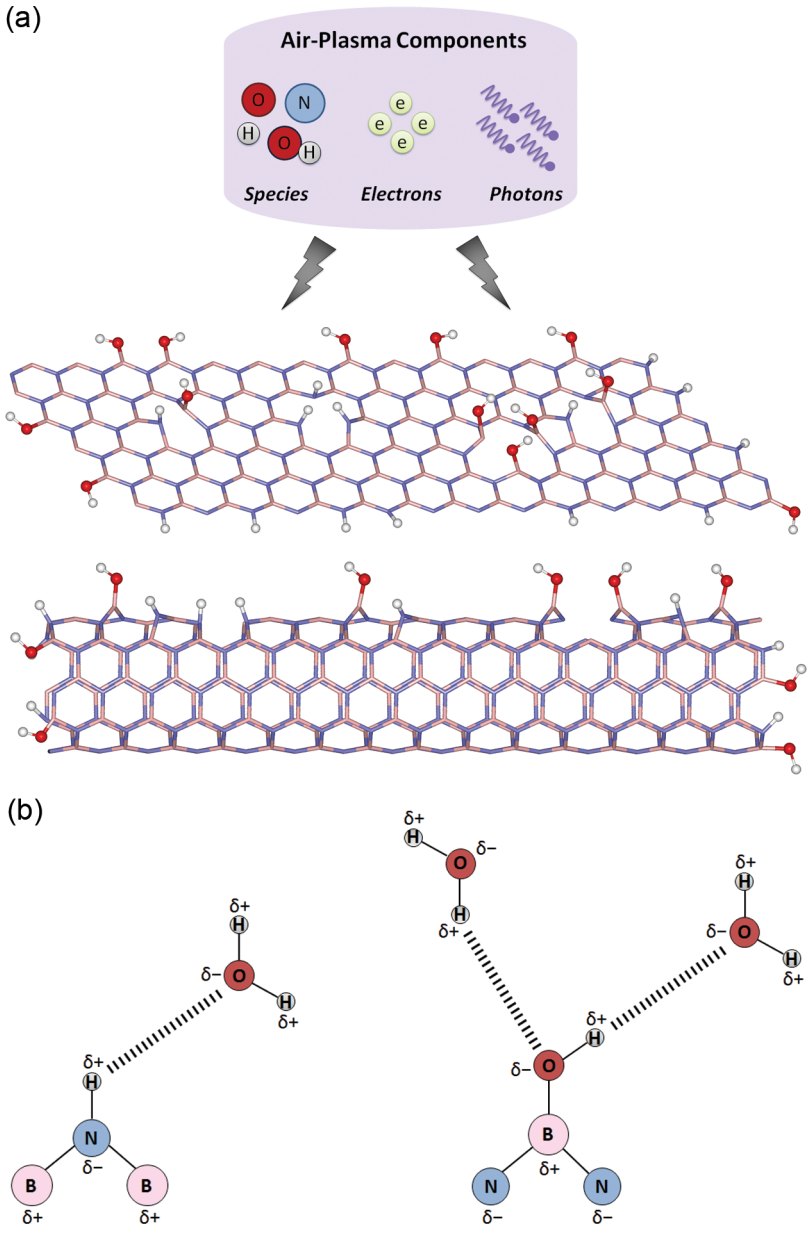

Figure 3. (a) Schematic representation of chemically engineered BN nanostructures by air-plasma treatment. The possible mechanisms for functionalization of BN nanosheets and nanotubes are bond formation at the edges (1), bond formation at defect sites, *e.g.*, vacancies (2), Lewis acid–base interactions (3), breakage of B–N bonds and forming new bonds (4). (b) Schematic representation of hydrogen bonds forming between water molecules and H-grafted nitrogen/OH-grafted boron atoms on the surface of the BN nanostructure films.

mask partially shields the film surface and interacts with the plasma components. Thus, plasma density decreases and a gradual penetration under the mask takes place. This provides control over the distribution of incident ions and reactive neutrals on the film surface.[32] On the basis of the plasma exposure level, three different areas existed on the sample: area I was fully exposed to the plasma for 10 min, while area II and area III were partially and fully covered by the canopy, respectively. Figure 4b shows O 1s spectra taken from these three areas under similar conditions (i.e., 400 μm spot size, 100 scans, Al Kα source, 0.1 eV energy step size). It is observed that the oxygen concentration on the partially covered area is much lower than that on the fully exposed area, indicating the presence of a hydroxyl gradient on the film surface. This can affect the wetting properties of the BN film. CA measurements in Figure 4c demonstrate superhydrophilicity in area I, hydrophobicity in area II, and superhydrophobicity in area III, which validate the possibility of creating fully or partly wettable patterns on the originally unwettable BN nanosheet film. Since water has a dipole moment of 1.85 D, the hydroxyl groups of the plasma-treated BN most likely interact with the positive polar components of water (-H groups) through hydrogen bonding.[33] Then, as the concentration of

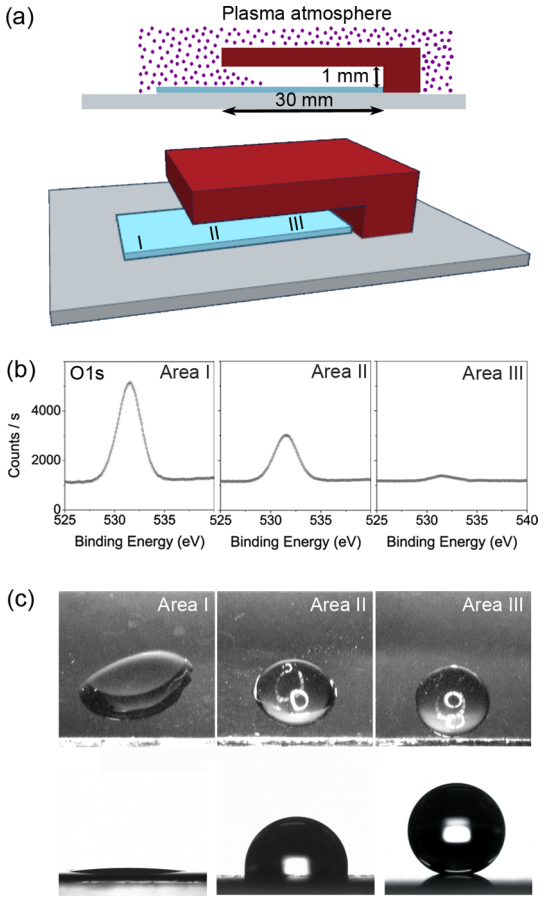

Figure 4. (a) Schematic illustration of masked plasma treatment resulting in three different areas on the BN nanosheet film: fully exposed to plasma (I), partially covered by the mask (II), and completely covered by the mask (III). (b) O 1s spectra taken from these three areas indicating a hydroxyl gradient resulting from the gradual decrease of the plasma density under the mask. (c) Images of water droplets at different areas of the film showing superhydrophilic, hydrophobic, and superhydrophobic properties.

hydroxyl groups increased on the surface, a higher number of hydrogen bonds and thus an extended wetting degree could be obtained. In other words, water droplets on the pristine BN nanostructure films initially exhibited the Cassie–Baxter state[34] in which the droplets are in partial contact with the tops of the rough surface features as well as the air pockets trapped between them. However, by applying the air-plasma treatment on the surfaces, water droplets exhibited the Wenzel state[35] in which the droplets can penetrate inside the surface features and be in full contact with the surface. Since the wetting transition from metastable Cassie–Baxter state to thermodynamically stable Wenzel state requires overcoming an energy barrier, it can be concluded that hydroxyl functionalization of the BN nanostructures acted like a catalyst to facilitate this process. It should be noted that the role of the energy barrier in wetting transition and the effect of external stimuli on the energy barrier reduction are broadly accepted facts.[36–42]

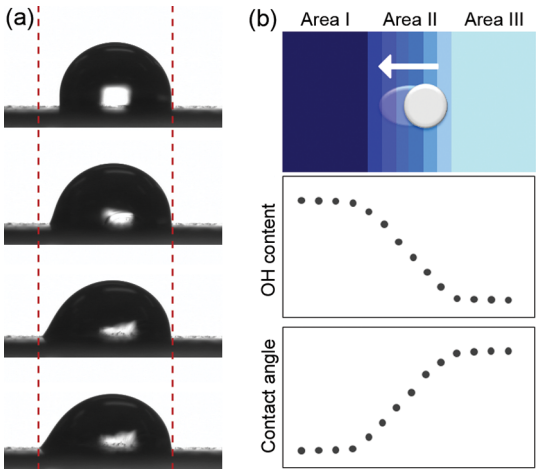

Figure 5. (a) Snapshots of a water droplet placed on area (II) of the graded BN nanosheet film indicating the spontaneous extension of the droplet over the film toward higher hydroxyl content (directional wetting); (b) schematic representation of directional water propagation on the chemically graded BN nanosheet film and schematic profiles of functionalization level and contact angle on its surface.

Another interesting feature observed in area II was the directional wetting along the chemical gradient on the BN nanosheet film. Figure 5a shows a series of images taken from a water droplet placed on area II of the graded BN nanosheet film. The droplet spontaneously extended over the film toward the direction of higher hydroxyl groups concentration (video, Supporting Information). Such dynamic propagation of the droplet on the chemically graded BN surface indicates the presence of a strong driving force for interactions of the liquid and the solid at the three-phase contact line, which can be described in terms of hydrophilicity augmentation along the direction of the functional group gradient. In fact, the grafted hydroxyl groups on the surface bring about larger surface energy and consequently elevated adhesion,[33] which promote propagation of water toward the areas of higher OH concentration (more hydrophilic areas), as schematically displayed in Figure 5b. This confirms that the CA value is a function of contact line chemical composition, and that the kinetics of droplet movement, rather than thermodynamics, dictate wettability.[43] To ensure that the driving force for droplet propagation was the chemical gradient (not an unleveled stage, for instance), the sample was rotated 180°, and the experiment was repeated. Again, the droplet propagated toward higher hydroxyl group concentration, demonstrating the concept of interface engineering to control surface wettability and liquid spreading along the chemical gradient on the BN film. Such directional wetting and control over liquid spreading can be of great interest in a broad range of applications such as surface-directed liquid flow, droplet-based microfluidics, DNA microarrays, capillary imbibition, fluidic optics, and inkjet printing.[1,3,6,44–46]

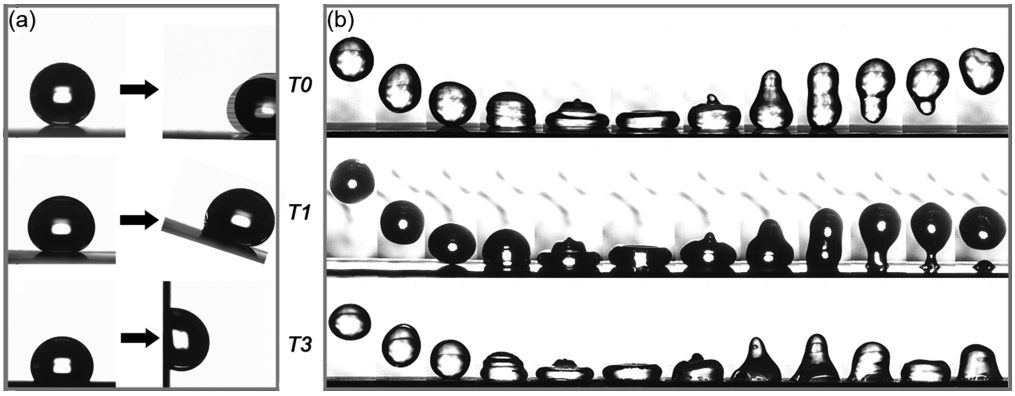

Figure 6. Dynamic wetting behavior of a BN nanosheet film in its pristine condition (T0) and after air-plasma treatment for 1 min (T1) and 3 min (T3): (a) snapshots of water droplets before and after tilting the film; (b) snapshots of water droplets impinging on the film.

Besides using a physical mask, the exposure time to plasma was another means to tune the functionalization level of the BN nanostructure films. Here we compare the dynamic properties of a BN nanosheet film in three stages: pristine and exposed to air plasma for 1 and 3 min (for simplicity, these stages will be referred to as T0, T1, and T3 respectively). Figure 6a demonstrates the "inclined surface" test results in which a water droplet was placed on the sample surface followed by tilting until the droplet began to move. The superhydrophobic film in T0 stage had a very low degree of sticking, and the water droplet moved as soon as the inclination of the film started (tilting degree $\theta_t < 1°$). The sample in T1 stage was also highly hydrophobic but showed a small level of stickiness. That is, during tilting the water droplet initially adhered to the surface and underwent some sliding and shape deformation (due to gravitational force) until θ_t reached 19° where the droplet quickly moved off the surface (more details in Figure S6, Supporting Information). The sample in T3 stage was much less hydrophobic; thus, the droplet pinned to the functionalized surface and did not move even when θ_t reached 90°. To further investigate the relation between surface functionalization level and the dynamic behavior of the droplets, a high-speed camera was used to record free-falling water droplets impacting on the BN film before and after air-plasma treatment. The successive snapshots in Figure 6b indicate that as the droplet hit the surface of the film in T0 stage, it deformed heavily and then bounced back from the surface with no observable liquid residue left. In fact, the large CA of the film allowed the droplet to store its kinetic energy in surface deformation and to be fully rebounded.[47] This confirmed the excellent water repellency of the BN nanosheet film in its pristine condition. However, since the BN film in the T1 stage was slightly less hydrophobic, a small portion of the droplet pinned to the surface during its rebound off the surface. In fact, intermolecular attractive forces between the slightly functionalized surface and the impinging liquid prevented the droplet from a complete bounce back.[48] This pinning effect became more pronounced when the water droplet hit the less hydrophobic surface in the T3 stage. The droplet then completely pinned to the hydroxidized surface and just oscillated before eventually coming to rest.

CONCLUSION

Air-plasma treatment was used for interface engineering of BN nanosheet and nanotube films to control their wetting properties. As a result, the edges, walls, and planes of the BN nanostructures could be hydroxyl-functionalized. The covalent grafting of hydroxyl groups on the BN nanostructures was verified using XPS, where in particular the formation of B—OH bonds rather than B—O bonds was confirmed, and the mechanisms for plasma functionalization of the BN nanostructures were explained.

The resulting hydroxyl-functionalized BN nanosheets and nanotube films showed a drastic change in their water-repellency. By tailoring the concentration of grafted hydroxyl groups, superhydrophilic, hydrophilic, and hydrophobic patterns were created on the initially superhydrophobic BN films. Such tunability in wetting properties of the BN films can be compared to that of some commercially available polymeric and organic coatings. Yet, the main advantage here is the robust mechanical properties and excellent thermal and chemical stability which make the BN films resistant to mechanical erosion, heat degradation, and many strong acids and bases.

Moreover, by controlling the interfacial interactions during the plasma treatment, a chemical gradient of hydroxyl groups on the BN nanostructure films was achieved which was then used to demonstrate directional-water-spreading functionality of the films. This can be of high technological importance, because currently most anisotropic and directional wetting surfaces are produced using expensive and complicated techniques creating asymmetric nanostructures on the surfaces, whereas the masked plasma process

utilized by us is relatively cheap and can easily be scaled up.

The herein presented controllable surface chemistry route provides further possibilities for the addition of other functional groups to the BN nanostructures, which for instance, can contribute to the poor interfacial contact and adhesion of BN/-metal and -polymer matrix nanocomposites,[49−51] improve BN nanostructure performance in biomedical research such as drug delivery and cancer therapy,[52] and promote their application in environmental research such as removal of oils, organic solvents, and dyes from water.[53]

MATERIALS AND METHODS

All chemicals of analytical grade were purchased from Wako Chemical Reagents Company (Japan), and were used without further purification.

Synthesis of BN Nanostructures. The CVD synthesis of the BN nanotube and nanosheet films was performed in an electric tube furnace, as described elsewhere.[17−20] In brief, the precursor powder materials (B/FeO/MgO) were mechanically mixed in a 2:1:1 molar ratio and were positioned in an alumina combustion boat covered with a Si/SiO_2 wafer. The boat was then set into an alumina test tube inside a vacuum chamber. The chamber was evacuated to 1 Torr, and then NH_3 gas was introduced at a rate of 0.4 mL/min. The precursors were heated to 1100 and 1300 °C, held for 60 min, and cooled to room temperature, and the produced BN nanosheet and nanotube films were removed from the furnace.

Plasma Treatment. BN nanostructure films were subject to direct ion/electron bombardment in a plasma generator device (SAKIGAKE-Semiconductor Co., Ltd., Japan) for 10 min. In this device, air was used to create the plasma. An AC voltage (8.5 kV, 20 kHz) was applied to the electrodes of the plasma device and the power was 45 W. The BN samples were placed on a processing stage under the plasma at ambient temperature and pressure. To create hydroxyl-group gradients on the BN nanostructure films, aluminum canopy masks were used with geometries illustrated in Figure 4.

Characterization. The morphology of the films was studied by a field-emission scanning electron microscope (FE-SEM; Hitachi SU8000, Japan), and their structures were analyzed by a high-resolution field emission transmission electron microscope (JEOL, JEM-2100F, Japan) equipped with an electron energy loss spectrometer (EELS). Auger electron spectroscopy (AES) was performed at room temperature using an AES thin film analyzer (ULVAC-PHI, Inc. Japan) with a cylindrical mirror analyzer and a thermal emission electron gun. X-ray photoelectron spectroscopy (XPS) analysis was performed using a monochromatic X-ray photoelectron spectrometer (Al Kα source, Thermo Scientific Theta Probe, USA), and the surface composition was determined by fitting the high resolution elemental spectra of the B 1s, N 1s, and O 1s peaks using the Thermo Scientific Avantage data acquisition and processing software. Interpretation of peak positions and binding energy shift was mainly performed by referring to *The Handbook of X-ray Photoelectron Spectroscopy*.[23]

Contact Angle (CA) Goniometry. Static and dynamic contact angle measurements were performed using an automated digital goniometer (DropMaster DM-701, KYOWA, Japan) equipped with a dispersing needle holder. Deionized water droplets of 3 μL volume were placed on the BN films with a microsyringe. CAs of three independent drops were averaged for each sample using FAMAS (interFAce Measurement & Analysis System) software version 2.4.5. (KYOWA, Japan). To investigate the dynamic behavior of free-falling water droplets on the films, a high-resolution high-speed camera (Phantom Miro eX2; Vision Research Inc., USA) with PCC (Phantom Camera Control) V2.14.727.0 software was utilized.

Conflict of Interest: The authors declare no competing financial interest.

Acknowledgment. This work was supported by the WPI Center for Materials Nanoarchitectonics (MANA) of the National Institute for Materials Science (NIMS; Tsukuba, Japan). The authors are grateful to Hiroshi Sonobe from "Nobby Tech. Ltd." (Tokyo, Japan) for high-speed camera imaging; and Chunyi Zhi, Masanori Mitome, Naoyuki Kawamoto, Tetsushi Taguchi, Keiko Yoshizawa, Daisuke Fujita, Nobuyuki Ishida, Carmen Perez Leon, Michiko Yoshitake, Toshihide Nabatame, Yutaka Misawa, and Hiroki Sugaya for technical support and fruitful discussions.

Supporting Information Available: Additional SEM images of the BN nanostructure films and their static CA measurement figures; structural and chemical characterization of BN nanostructures by TEM and XPS; dynamic wetting behavior of BN nanostructure films. This material is available free of charge *via* the Internet at http://pubs.acs.org.

REFERENCES AND NOTES

1. Xia, D. Y.; Johnson, L. M.; Lopez, G. P. Anisotropic Wetting Surfaces with One-Dimesional and Directional Structures: Fabrication Approaches, Wetting Properties and Potential Applications. *Adv. Mater.* **2012**, *24*, 1287–1302.
2. Barthlott, W.; Neinhuis, C. Purity of the Sacred Lotus, or Escape from Contamination in Biological Surfaces. *Planta* **1997**, *202*, 1–8.
3. Liimatainen, V.; Sariola, V.; Zhou, Q. Controlling Liquid Spreading Using Microfabricated Undercut Edges. *Adv. Mater.* **2013**, *25*, 2275–2278.
4. Chung, J. Y.; Youngblood, J. P.; Stafford, C. M. Anisotropic Wetting on Tunable Micro-Wrinkled Surfaces. *Soft Matter* **2007**, *3*, 1163–1169.
5. Kooij, E. S.; Jansen, H. P.; Bliznyuk, O.; Poelsema, B.; Zandvliet, H. J. W. Directional Wetting on Chemically Patterned Substrates. *Colloid Surf. A* **2012**, *413*, 328–333.
6. Jokinen, V.; Leinikka, M.; Franssila, S. Microstructured Surfaces for Directional Wetting. *Adv. Mater.* **2009**, *21*, 4835–4838.
7. Tawfick, S.; De Volder, M.; Copic, D.; Park, S. J.; Oliver, C. R.; Polsen, E. S.; Roberts, M. J.; Hart, A. J. Engineering of Micro- and Nanostructured Surfaces with Anisotropic Geometries and Properties. *Adv. Mater.* **2012**, *24*, 1628–1674.
8. Bahr, J. L.; Yang, J. P.; Kosynkin, D. V.; Bronikowski, M. J.; Smalley, R. E.; Tour, J. M. Functionalization of Carbon Nanotubes by Electrochemical Reduction of Aryl Diazonium Salts: A Bucky Paper Electrode. *J. Am. Chem. Soc.* **2001**, *123*, 6536–6542.
9. Cao, L.; Chen, H. Z.; Wang, M.; Sun, J. Z.; Zhang, X. B.; Kong, F. Z. Photoconductivity Study of Modified Carbon Nanotube/Oxotitanium Phthalocyanine Composites. *J. Phys. Chem. B* **2002**, *106*, 8971–8975.
10. Konya, Z.; Vesselenyi, I.; Niesz, K.; Kukovecz, A.; Demortier, A.; Fonseca, A.; Delhalle, J.; Mekhalif, Z.; Nagy, J. B.; Koos, A. A.; *et al.* Large Scale Production of Short Functionalized Carbon Nanotubes. *Chem. Phys. Lett.* **2002**, *360*, 429–435.
11. Plank, N. O. V.; Jiang, L. D.; Cheung, R. Fluorination of Carbon Nanotubes in CF_4 Plasma. *Appl. Phys. Lett.* **2003**, *83*, 2426–2428.
12. Felten, A.; Bittencourt, C.; Pireaux, J. J.; Van Lier, G.; Charlier, J. C. Radio-Frequency Plasma Functionalization of Carbon Nanotubes Surface O_2, NH_3, and CF_4 Treatments. *J. Appl. Phys.* **2005**, *98*, 074308.
13. Pakdel, A.; Zhi, C. Y.; Bando, Y.; Golberg, D. Low-Dimensional Boron Nitride Nanomaterials. *Mater. Today* **2012**, *15*, 256–265.

14. Pakdel, A.; Bando, Y.; Golberg, D. Nano Boron Nitride Flatland. *Chem. Soc. Rev.* **2014**, *43*, 934–959.
15. Lee, C. H.; Drelich, J.; Yap, Y. K. Superhydrophobicity of Boron Nitride Nanotubes Grown on Silicon Substrates. *Langmuir* **2009**, *25*, 4853–4860.
16. Li, L. H.; Chen, Y. Superhydrophobic Properties of Non-aligned Boron Nitride Nanotube Films. *Langmuir* **2010**, *26*, 5135–5140.
17. Pakdel, A.; Zhi, C. Y.; Bando, Y.; Nakayama, T.; Golberg, D. Boron Nitride Nanosheet Coatings with Controllable Water Repellency. *ACS Nano* **2011**, *5*, 6507–6515.
18. Pakdel, A.; Wang, X. B.; Bando, Y.; Golberg, D. Nonwetting "White Graphene" Films. *Acta Mater.* **2013**, *61*, 1266–1273.
19. Pakdel, A.; Bando, Y.; Golberg, D. Morphology-Driven Nonwettability of Nanostructured BN Surfaces. *Langmuir* **2013**, *29*, 7529–7533.
20. Pakdel, A.; Zhi, C. Y.; Bando, Y.; Nakayama, T.; Golberg, D. A Comprehensive Analysis of the CVD Growth of Boron Nitride Nanotubes. *Nanotechnology* **2012**, *23*, 215610.
21. Boinovich, L. B.; Emelyanenko, A. M.; Pashinin, A. S.; Lee, C. H.; Drelich, J.; Yap, Y. K. Origins of Thermodynamically Stable Superhydrophobicity of Boron Nitride Nanotubes Coatings. *Langmuir* **2012**, *28*, 1206–1216.
22. Pakdel, A.; Wang, X. B.; Zhi, C. Y.; Bando, Y.; Watanabe, K.; Sekiguchi, T.; Nakayama, T.; Golberg, D. Facile Synthesis of Vertically Aligned Hexagonal Boron Nitride Nanosheets Hybridized with Graphitic Domains. *J. Mater. Chem.* **2012**, *22*, 4818–4824.
23. Moulder, J. F.; Stickle, W. F.; Sobol, P. E.; Bomben, K. D. *The Handbook of X-Ray Photoelectron Spectroscopy*; ULVAC-PHI, Inc.: Chigasaki, 1995.
24. *NIST X-ray Photoelectron Spectroscopy Database*, version 4.1; National Institute of Standards and Technology: Gaithersburg, MD, **2012**, http://srdata.nist.gov/xps/.
25. Sainsbury, T.; Satti, A.; May, P.; Wang, Z. M.; McGovern, I.; Gun'ko, Y. K.; Coleman, J. Oxygen Radical Functionalization of Boron Nitride Nanosheets. *J. Am. Chem. Soc.* **2012**, *134*, 18758–18771.
26. Giovambattista, N.; Debenedetti, P. G.; Rossky, P. J. Effect of Surface Polarity on Water Contact Angle and Interfacial Hydration Structure. *J. Phys. Chem. B* **2007**, *111*, 9581–9587.
27. Lee, S. H.; Rossky, P. J. A Comparison of the Structure and Dynamics of Liquid Water at Hydrophobic and Hydrophilic Surfaces —A Molecular-Dynamics Simulation Study. *J. Chem. Phys.* **1994**, *100*, 3334–3345.
28. Moon, O. M.; Kang, B. C.; Lee, S. B.; Boo, J. H. Temperature Effect on Structural Properties of Boron Oxide Thin Films Deposited by the MOCVD Method. *Thin Solid Films* **2004**, *464*, 164–169.
29. Lin, Y.; Williams, T. V.; Xu, T. B.; Cao, W.; Elsayed-Ali, H. E.; Connell, J. W. Aqueous Dispersions of Few-Layered and Monolayered Hexagonal Boron Nitride Nanosheets from Sonication-Assisted Hydrolysis: Critical Role of Water. *J. Phys. Chem. C* **2011**, *115*, 2679–2685.
30. Zhi, C. Y.; Bando, Y.; Terao, T.; Tang, C. C.; Kuwahara, H.; Golberg, D. Chemically Activated Boron Nitride Nanotubes. *Chem.—Asian J.* **2009**, *4*, 1536–1540.
31. Ciofani, G.; Genchi, G. G.; Liakos, I.; Athanassiou, A.; Dinucci, D.; Chiellini, F.; Mattoli, V. A Simple Approach to Covalent Functionalization of Boron Nitride Nanotubes. *J. Colloid Interface Sci.* **2012**, *374*, 308–314.
32. Zheng, L.; Ling, L.; Hua, X.; Oehrlein, G. S.; Hudson, E. A. Studies of Film Deposition in Fluorocarbon Plasmas Employing a Small Gap Structure. *J. Vac. Sci. Technol. A* **2005**, *23*, 634–642.
33. Hernandez, S. C.; Bennett, C. J. C.; Junkermeier, C. E.; Tsoi, S. D.; Bezares, F. J.; Stine, R.; Robinson, J. T.; Lock, E. H.; Boris, D. R.; Pate, B. D.; *et al*. Chemical Gradients on Graphene to Drive Droplet Motion. *ACS Nano* **2013**, *7*, 4746–4755.
34. Cassie, A. B. D.; Baxter, S. Wettability of Porous Surfaces. *Trans. Faraday Soc.* **1944**, *40*, 546–551.
35. Wenzel, R. N. Resistance of Solid Surfaces to Wetting by Water. *Ind. Eng. Chem.* **1936**, *28*, 988–994.
36. Ishino, C.; Okumura, K.; Quere, D. Wetting Transitions on Rough Surfaces. *Europhys. Lett.* **2004**, *68*, 419–425.
37. Bomiashenko, E.; Musin, A.; Whyman, G.; Zinigrad, M. Wetting Transitions and Depinning of the Triple Line. *Langmuir* **2012**, *28*, 3460–3464.
38. Giacomello, A.; Meloni, S.; Chinappi, M.; Casciola, C. M. Cassie–Baxter and Wenzel States on a Nanostructured Surface: Phase Diagram, Metastabilities, and Transition Mechanism by Atomistic Free Energy Calculations. *Langmuir* **2012**, *28*, 10764–10772.
39. Lafuma, A.; Quere, D. Superhydrophobic States. *Nat. Mater.* **2003**, *2*, 457–460.
40. Sbragaglia, M.; Peters, A. M.; Pirat, C.; Borkent, B. M.; Lammertink, R. G. H.; Wessling, M.; Lohse, D. Spontaneous Breakdown of Superhydrophobicity. *Phys. Rev. Lett.* **2007**, *99*, 156001.
41. Murakami, D.; Jinnai, H.; Takahara, A. Wetting Transition from the Cassie–Baxter State to the Wenzel State on Textured Polymer Surfaces. *Langmuir* **2014**, *30*, 2061–2067.
42. Koishi, T.; Yasuoka, K.; Fujikawa, S.; Ebisuzaki, T.; Zeng, X. C. Coexistence and Transition between Cassie and Wenzel State on Pillared Hydrophobic Surface. *Proc. Natl. Acad. Sci. U.S.A.* **2009**, *106*, 8435–8440.
43. Gao, L. C.; McCarthy, T. J. How Wenzel and Cassie Were Wrong. *Langmuir* **2007**, *23*, 3762–3765.
44. Chu, K. H.; Xiao, R.; Wang, E. N. Uni-directional Liquid Spreading on Asymmetric Nanostructured Surfaces. *Nat. Mater.* **2010**, *9*, 413–417.
45. Chiou, N. R.; Lui, C. M.; Guan, J. J.; Lee, L. J.; Epstein, A. J. Growth and Alignment of Polyaniline Nanofibres with Superhydrophobic, Superhydrophilic and Other Properties. *Nat. Nanotechnol.* **2007**, *2*, 354–357.
46. Kim, E.; Whitesides, G. M. Imbibition and Flow of Wetting Liquids in Noncircular Capillaries. *J. Phys. Chem. B* **1997**, *101*, 855–863.
47. Callies, M.; Quere, D. On Water Repellency. *Soft Matter* **2005**, *1*, 55–61.
48. Aria, A. I.; Gharib, M. Reversible Tuning of the Wettability of Carbon Nanotube Arrays: The Effect of Ultraviolet/Ozone and Vacuum Pyrolysis Treatments. *Langmuir* **2011**, *27*, 9005–9011.
49. Yamaguchi, M.; Pakdel, A.; Zhi, C. Y.; Bando, Y.; Tang, D. M.; Faerstein, K.; Shtansky, D.; Golberg, D. Utilization of Multi-walled Boron Nitride Nanotubes for the Reinforcement of Lightweight Aluminum Ribbons. *Nanoscale Res. Lett.* **2013**, *8*, 3.
50. Wang, X. B.; Pakdel, A.; Zhang, J.; Weng, Q. H.; Zhai, T. Y.; Zhi, C. Y.; Golberg, D.; Bando, Y. Large-Surface-Area BN Nanosheets and Their Utilization in Polymeric Composites with Improved Thermal and Dielectric Properties. *Nanoscale Res. Lett.* **2012**, *7*, 662.
51. Zhi, C. Y.; Bando, Y.; Tang, C. C.; Kuwahara, H.; Golberg, D. Large-Scale Fabrication of Boron Nitride Nanosheets and Their Utilization in Polymeric Composites with Improved Thermal and Mechanical Properties. *Adv. Mater.* **2009**, *21*, 2889–2893.
52. Li, X.; Hanagata, N.; Wang, X. B.; Yamaguchi, M.; Yi, W.; Bando, Y.; Golberg, D. Multimodal Luminescent-Magnetic Boron Nitride Nanotubes@$NaGdF_4$:Eu Structures for Cancer Therapy. *Chem. Commun.* **2014**, *50*, 4371–4374.
53. Lei, W. W.; Portehault, D.; Liu, D.; Qin, S.; Chen, Y. Porous Boron Nitride Nanosheets for Effective Water Cleaning. *Nat. Commun.* **2013**, *4*, 1777.